FIRST STEPS IN DEVELOPMENT OF A TRANSLATIONAL NON EQUILIBRIUM MODEL USING MAXIMUM ENTROPY PRINCIPLE

BY

VEGNESH JAYARAMAN

THESIS

Submitted in partial fulfillment of the requirements
for the degree of Master of Science in Aerospace Engineering
in the Graduate College of the
University of Illinois at Urbana-Champaign, 2019

Urbana, Illinois

Adviser:

Associate Professor Marco Panesi

ABSTRACT

This thesis elaborates the steps taken in the development of a model for flows that are in translational non-equilibrium. The backbone of the model relies on Boltzmann equation for gases as a starting point. Three mathematical tools - domain decomposition, moment methods similar to method of weighted residuals and maximum entropy principle are used for defining the model and developing the underlying governing equations. The underlying modeling goal was to serve as a bridge in terms of computational cost and accuracy, between high fidelity Boltzmann equations and empirically driven Navier Stokes equations. The model effectiveness is studied by solving numerically discretized model equations for one dimensional setting . The problem studied is that of a normal shock occurring in a monoatomic gas. The various assumptions, validation tools used and problems associated with model development are elaborated.

Mind, a beautiful servant, but a dangerous master.

ACKNOWLEDGMENTS

In the time I have spent at UIUC, I have had a chance to meet, interact and learn from a number of individuals. Firstly, I would like to thank Prof. Marco Panesi for giving me the opportunity to work with him and for funding my work. He is a brilliant person and I am grateful for getting the opportunity to work with him. Next, I would like to thank Dr. Yen Liu from NASA Ames Research Center for his ideas and guidance through the project. My interactions with Dr. Alessandro Munafo and Dr. Bruno Lopez have made me realize the expertise in programming and physics required in an excellent researcher and I am indebted to them for that. I would like to express my gratitude to my fellow NEQRAD group members who have moulded my thought process over the years. I am excited to see the great leaps that all of you make in your careers going forward. Finally, I would like to thank my friends and family to have made my stay in UIUC memorable.

TABLE OF CONTENTS

LIST OF FIGURES

CHAPTER 1

INTRODUCTION

The flow around the body of a re-entry vehicle widely differs in the different flight regimes of the vehicle. Specifically, (re)entry of a vehicle into the atmosphere of a heavenly body occurs at vehicle speeds above 5 times the value of the local speed of sound. At these speeds, a strong bow shock is created in front of the vehicle and the pressure, temperature and composition of gases on either side of the shock is widely different. In addition, the atmosphere around the vehicle is typically rarefied. As a result, there is a interplay o between aerodynamics, thermodynamics and material physical processes due to the high speeds involved [1]. Some of physical phenomena that occur during re-entry are shown in Figure 1.1

Particularly of interest is the way thermodynamics of the gases surrounding the vehicle affect the vehicle surface and flight characteristics. The way energy is stored in gases is through their motion (translation) and internal states (rotation and vibration modes in cases of molecules, electronic modes for all gases). In this work, we wish to isolate the study of motion of gas molecules and the methods through which they affect bulk properties like pressure, temperature and flow velocity.

In general, the Navier Stokes equations are used for modelling the flow around bodies. The underlying assumptions of Navier stokes models (velocity distribution of gases is a perturbed equilibrium distribution) are not valid in rarefied hypersonic flows. The translational and internal energy modes of the gas are not in equilibrium. This is because the relaxation time of gas molecules (a measure of time taken to reach equilibrium) is of the same order as the flow characteristic time. Equivalently, from a statistical perspective, the energy distribution of gas molecules is largely different from that of the expected equilibrium distribution. In these regimes, one of the best ways to describe flow processes is through the use of a statistical description based on kinetic theory of gases.

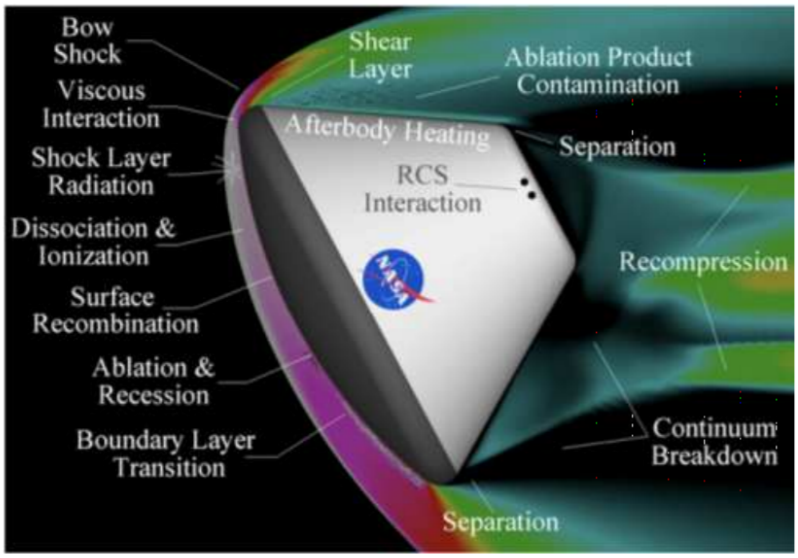

Figure 1.1: Hypersonic Re-entry Flowfield - Source: NASA

Statistical models, while robust at describing physical phenomena, are computationally expensive to solve. For example, the Boltzmann equation, which is the governing equation describing the evolution of the distribution of molecular velocities[2, 3], is a 7 dimensional equation (6D in phase space and 1D in time). The curse of dimensionality makes numerical models slow and resource hungry.

The goal of the current work is to develop a model that acts like a bridge between low fidelity-fast Navier Stokes equations and high fidelity-slow Boltzmann equations. We draw inspiration from these extreme models and develop a model framework that is able to provide robust solutions that do not have simplifying assumptions like Navier Stokes and give solutions within a tractable time.

1.1 Relevant Literature

Multiple numerical techniques exist to numerically solve the Boltzmann equation. From a deterministic perspective, finite difference [4], finite volume [5] or Galerkin techniques [6] have been developed which are similar to techniques used for numerically solving Navier Stokes equations. The direct simulation Monte Carlo method provides a probabilistic alternative [7].

Another way to tackle the problem is using the method of weighted residuals and derive macroscopic moment equations. The idea of using moment methods for obtaining solutions to the Boltzmann equation was introduced by Grad [8]. Levermore[9] introduced a maximum entropy based closure for such methods. Analysis has shown that these methods are prone to yield non physical solutions in certain cases.[10, 11]. Additionally, for obtaining numerical solutions, boundary conditions need to be specified for higher order moments like heat flux. This may not be available for all physical problems. In all of these methods, the entire velocity space is considered for obtaining the macroscopic model.

The approach proposed here is to solve for the moments of the Boltzmann equation. The key difference between the previous moments based methods and the current method is that the solution is sought, in a piecewise manner, over a limited range of the velocity space. The velocity domain is decomposed into small groups, and the velocity distribution function in each of these groups is reconstructed using group macroscopic quantities as constraints and functions generated using the maximum entropy principle. The macroscopic governing equations are obtained by using the method of weighted residuals and the Boltzamann's equation. A similar model has been derived earlier for modeling thermo-chemical non-equilibrium [12, 10].

Some existing approaches that are similar to the model proposed here are : a hybrid-kinetic approach that assumes a Maxwellian distribution in a certain region of velocity space and solves the kinetic equation in the rest of the velocity space[13] and a model for the specific case of two groups using methods similar to the one suggested in current work[14]. To the best of our knowledge, this is the first attempt to implement such a model for an arbitrary number of groups.

1.2 Thesis Outline

The thesis is divided into four chapters. The first chapter gives an overview of the Boltzmann equation and Navier Stokes equations and provides details on some of the numerical methods used to solve the Boltzmann Equation. In the next chapter, the model governing equations are derived. Following this, the numerical framework for solving the model is provided and some results

are presented. In the last chapter, the key challenges, pitfalls, concluding thought and future directions are suggested. Some of the work elaborated here was presented by the author earlier[15].

CHAPTER 2

BOLTZMANN EQUATION

The most common model used for simulating flows are the Navier Stokes equations. The equations can be written as :

$$\frac{\partial \rho}{\partial t} + \nabla.(\rho \vec{V}) = 0 \tag{2.1}$$

$$\frac{\partial \rho V_i}{\partial t} + \nabla.(\rho \vec{V} V_i) = -\frac{\partial P}{\partial x_i} + \frac{\partial \tau_{ij}}{\partial x_i} + \rho F_i \tag{2.2}$$

$$\frac{\partial \rho e + \frac{1}{2}\rho V^2}{\partial t} + \nabla.(\rho \vec{V}(h + \frac{1}{2}V^2)) = \nabla.(\tau.\vec{V} - \vec{q}) + \rho \vec{F}.\vec{V} \tag{2.3}$$

ρ is the density of the gas, V is the velocity, τ is the viscous stress, $\vec{F}$ is the external force, P is pressure, e is specific internal energy, h is the enthalpy and $\vec{q}$ is the heat flux.

Even for simple problems, the above set of equations cannot be solved. One of the major reasons is the presence of τ and $\vec{q}$ terms. In general, constitutive relations are empirically developed for viscous stress and heat flux which depend on the velocity gradient and temperature gradient respectively. There are significant assumptions made while developing these relations and these assumptions are typically invalid when considering the flows that occur in re-entry. A statistical description is will be able to circumvent some of the assumptions and additionally, the need for empirical measurements to model viscous stress and heat flux terms.

2.1 Boltzmann Equation

The Boltzmann equation models the rate of change of the velocity distribution function of the molecules in phase space with respect to position and

time. It provides statistical description of the dynamics of the particles that constitute a gas. The equations expressed here closely follow the derivation given in "Introduction to Physical Gas Dynamics" [2]

The Boltzmann equation can be written as:

$$\left(\frac{\partial f}{\partial t} + \vec{c}.\frac{\partial f}{\partial \vec{x}} + \frac{\partial \vec{F} f}{\partial \vec{c}}\right) = \tag{2.4}$$

$$\int_{-\infty}^{\infty} \int_{dP_c} [f(\vec{c}', \vec{x}, t) f(\vec{v}', \vec{x}, t) - f(\vec{c}, \vec{x}, t) f(\vec{v}, \vec{x}, t)] g dP_c dV_v$$

$f = f(\vec{(c)}, \vec{x}, t)$ is the un-normalized velocity distribution function, $\vec{F}$ is the external force acting on objects, $\vec{x}$ is the position, $\vec{c}, \vec{c}', \vec{v}, \vec{v}'$ are variables representing the molecular velocities, g is the relative speed and dP_c is the differential cross section.

The first term represent the change in distribution function with time keeping other parameters constant, the second and third terms represent the flux of distribution function in the physical and velocity space. In the integral on the right side of 2.5, there are two terms. The first term represents the replenishing collisions between molecules and the second term represents depleting collisions.

Some of the key assumptions used in the derivation of Boltzmann equations are[2]: there are enough molecules in the gas to warrant a statistical description, the range of intermolecular forces is very small in comparison to the average distance travelled by molecules, binary collisions, no correlations between the velocities of colliding molecules and the distribution function remains roughly constant over the duration of the collision.

By taking velocity moments of equation -2.5 and integrating over the entire velocity space , the Navier Stokes equations 2.1, 2.2, 2.3 can be obtained. Specifically the zeroth velocity moment corresponds to conservation of mass, the first velocity moment corresponds to conservation of momentum and second velocity moment corresponds to conservation of energy. Furthermore, mass, momentum and total energy are collision in-variants, these moments of the right side of the Boltzmann equation integrate out to zero. In addition, if an appropriate collision cross section is chosen, the expressions for viscosity and thermal conductivity can be directly obtained without empiri-

cal measurements.

2.2 Equilibrium Distribution

A necessary and sufficient condition for equilibrium is given by [2]:

$$f(\vec{c}', \vec{x}, t) f(\vec{v}', \vec{x}, t) = f(\vec{c}, \vec{x}, t) f(\vec{v}, \vec{x}, t) \tag{2.5}$$

Using the above condition and definition of temperature, the Maxwell distribution function - which corresponds to the equilibrium velocity distribution is given by:

$$F_m(\vec{c}) = n \left(\frac{m}{2\pi k T} \right)^{\frac{3}{2}} \exp\left(-\frac{m}{2kT} |\vec{c} - \vec{V}|^2 \right) \tag{2.6}$$

Here, n is the number density of molecules, m is the mass of the molecule, T is the temperature and k is the Boltzmann constant.

If equilibrium assumption is used, and the flow governing equations are obtained using the the integrated velocity moments of Boltzmann equation, we obtain the unsteady Euler equations. These do not have viscous stresses and heat flux terms.

From the above analysis, one of the key observations is the fact that, viscous stresses and heat flux are artifacts of non-equilibrium processes. In case strong non-equilibrium occurs, empirical constitutive models will fail to capture the underlying physics. This is because Navier Stokes equations are obtained when the moments of the Boltzmann equation are obtain with the assumption that the underlying distribution is a perturbed Maxwellian. It would be better to solve the Boltzmann equations, instead of Navier Stokes equations to capture the underlying physics.

2.2.1 BGK model

Non-linear collision terms in the right side of Eq.2.5 are pose a significant challenge for most numerical models. The Bhatnagar-Gross-Krook[16] (BGK) is an alternative simplified approximation to the collision integral.

The collision terms, based on the BGK model, can be expressed as[17] :

$$\left(\frac{\partial f}{\partial t}\right)_{collision} = \nu(F_m - f) \tag{2.7}$$

The variable ν is a collision frequency depends on the state of the gas and the number density but not on the molecular velocity[2]. F_m is the local Maxwellian distribution. The local density, velocity and temperature are obtained by taking the velocity moments of the distribution function:

$$\rho = \int_{\vec{c}} m f d\vec{c} \tag{2.8}$$

$$\rho\vec{V} = \int_{\vec{c}} \vec{c} f d\vec{c} \tag{2.9}$$

$$2RT = \frac{1}{\beta} = \frac{2}{3n}\int m(\vec{c} - \vec{u})^2 f d\vec{c} \tag{2.10}$$

R is the gas constant.

The collision that deplete the distribution are represented by the $-\nu f$ term, and the effect of replenishing collisions are expressed using νF_M. BGK model effectively states that the molecules are undergoing a relaxation process to a Maxwellian distribution at the local mean velocity, density and temperature. It is shown that the BGK model assumption hold true for the case of Maxwell molecules and rigid spheres [2, 17]

The Krook equation is the Boltzmann equation obtained by replacing the collision term in equation Eq.(2.5) with the BGK collision model terms. In this work, we consider a Krook model as the baseline statistical model. Further, we assume there are no external forces acting on the gases. Using the above simplifications, the Krook model can be expressed as :

$$\left(\frac{\partial f}{\partial t} + \vec{c}.\frac{\partial f}{\partial \vec{x}}\right) = \nu(F_m - f) \tag{2.11}$$

The Krook Equation, looks like a linear partial differential equation, but it is not. Effects of the collision frequency term and the Maxwellian distribution make the Krook equation non-linear in nature. However, solution to Krook equation is far simpler than the full Boltzmann equation

CHAPTER 3

MATHEMATICAL FORMULATION

In this chapter, the steps taken in developing the model are elaborated. The underlying principles that the model tries to exploit are:

- Dividing the velocity space into multiple bins/groups
- Assume a functional form for the distribution function within each of these groups
- Use the Boltzmann equation and the functional form defined earlier to generate governing equations for macroscopic quantities like density, velocity and temperature

The key innovations of the current model, over other methods that model the Boltzmann equations are:

- Use of maximum entropy principle to generate the functional form of distribution within each group
- Modeling the moments of the Boltzmann equation

In the following sections, model development, mathematical formulations and the advantages of the model are elaborated.

3.1 Group Distribution Function

Maximum entropy principle is used in information theory [18, 19], as interpolants[20], and as a method for providing solutions to under-determined inverse problems [21].

In thermodynamics, the entropy of a system is maximized when it reaches an equilibrium state. This property is exploited in statistical mechanics and kinetic theory to obtain the energy and velocity distribution of particles at

a particular temperature. The collision integral for a bimolecular collision in Boltzmann equation is given as [2] :

$$\left[\frac{\partial}{\partial t}(f)\right]_{coll} = \int_{-\infty}^{\infty} \int_{dP_c} [f(\vec{c}', \vec{x}, t) f(\vec{v}', \vec{x}, t) - f(\vec{c}, \vec{x}, t) f(\vec{v}, \vec{x}, t)] g dP_c dV_v \quad (3.1)$$

A necessary and sufficient condition for equilibrium is given by [2]:

$$f(\vec{c}')f(\vec{v}') = f(\vec{c})f(\vec{v}) \quad (3.2)$$

$$\ln(f(\vec{c}')) + \ln(f(\vec{c}')) = \ln(f(\vec{c})) + \ln(f(\vec{c}')) \quad (3.3)$$

From Eq.(3.3), it is observed that $\ln(f)$ is a collisional invariant. For an elastic collision, the total mass, the total linear momentum and the total mechanical energy are conserved in a collision. Using this fact, $\ln(f)$ is expressed as linear combination of the collisional invariants from classical mechanics.

$$\ln(f(\vec{c})) = \alpha + \vec{\gamma}.\vec{c} + \delta \vec{c}.\vec{c} \quad (3.4)$$

On invoking the maximum entropy principle over the entire velocity space, the expression 2.6 is obtained. In the current model, the maximum entropy principle is invoked within each velocity group to obtain an expression for the distribution valid only within that group.

The mathematical formulation for obtaining the group distribution function can be stated as[15]: Obtain a function f_k such that entropy of this function is maximized and the first 3 velocity moments of f_k are equal to a given value of the moments $(\mu_{n,k})$ where $n = 0, 1, 2$ corresponds to the order of the moment. k represent the index used to number each group in the velocity space. The maximum entropy functional can be defined as:

$$\mathcal{J}[f_k] = \int_{\vec{c}_k}^{\vec{c}_{k+1}} \left(-f_k \ln f_k + f_k + \alpha_k f_k + \vec{\gamma}_k.\vec{c} f_k + \delta_k c^2 f_k\right) d\vec{c} - \alpha_k \mu_{0,k} - \vec{\gamma}_k.\vec{\mu}_{1,k} - \delta \mu_{2,k} \quad (3.5)$$

where α_k, $\vec{\gamma}_k$ and δ_k are the Lagrange multipliers. $\vec{c}$ is the velocity vector corresponding to the three dimensions in velocity space. The moments are

defined as:

$$\mu_{0,k} = \int_{\vec{c}_k}^{\vec{c}_{k+1}} f_k d\vec{c} \tag{3.6}$$

$$\vec{\mu}_{1,k} = \int_{\vec{c}_k}^{\vec{c}_{k+1}} \vec{c} f_k d\vec{c} \tag{3.7}$$

$$\mu_{2,k} = \int_{\vec{c}_k}^{\vec{c}_{k+1}} c^2 f_k d\vec{c} \tag{3.8}$$

The functional variation of equation (3.5) results in:

$$\ln(f_k) = \alpha_k + \vec{\gamma}_k.\vec{c} + \delta_k \vec{c}.\vec{c} \tag{3.9}$$

The expression for the distribution function is given by:

$$f(\vec{x}, t; \vec{c}) = \sum_{k=1}^{k=N_g} f_k(\vec{x}, t; \vec{c}) \tag{3.10}$$

$$f_k(\vec{x}, t; \vec{c}) = \begin{cases} A_k \exp(-\beta_k(\vec{c} - \vec{w_k})^2), & \text{if } \vec{c}_k \leq \vec{c} \leq \vec{c}_{k+1} \\ 0, & \text{otherwise} \end{cases} \tag{3.11}$$

where k is the group index, N_g is the number of velocity groups, c_k and c_{k+1} are the k^{th} group's lower and upper velocity bounds and A_k, β_k and w_k are the function parameters. The variation of group macroscopic quantities in space and time are encoded within the group function parameters. Equations (3.9) and (3.11) are equivalent mathematical expressions.

Eq.(3.11) is used as an approximation of the velocity distribution function within each velocity group. This formulation effectively states the gas particles in a particular group are in local equilibrium. They can be in non-equilibrium with gas molecules in another group. The schematic for model formulation, illustrating the velocity groups and the distribution function within each group, is shown in Figure 3.1.

This concludes the first major component of the model - the function formulation. The two concepts of dividing a velocity space into groups and assuming a function expression within each group is not unique. When a finite difference approximation is used to solve the Boltzmann equation directly,

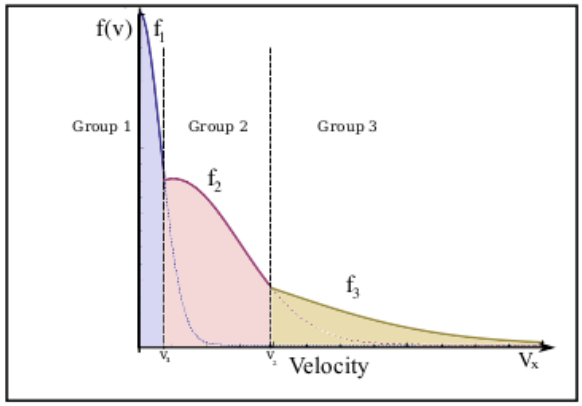

Figure 3.1: Piecewise representation of velocity distribution function using 3 groups.

the function formulation for the velocity distribution within the discretized velocity domain is assumed to be a polynomial. Similarly, in finite element methods for solving Boltzmann equation, discretization of velocity space is performed and linear combinations of basis functions are used within each discrete space to model the function.

The motivation for choosing a maximum entropy formulation for the function approximation is two fold, entropy maximization has a physical implication in thermodynamics, secondly, at equilibrium, the entire distribution can be represented by just three parameters.

3.2 Model Governing Equations

The second aspect of the model involves using the function formulation and Boltzmann equations to derive the model governing equations. Specifically, the velocity moments of the Krook equation 2.11 is used for obtaining the model equations. The focus of the current work is to study the behaviour of the model in zero dimensional and one dimensional space and three or one dimensions in velocity space. No external forces are assumed to act on the system.

In the current work, macroscopic fluid flow is assumed to be only along the x direction. the profile is considered to be a Maxwellian at the instantaneous local temperature with zero mean flow along the y and z direction. The

group distribution function that is taken for all cases is given by:

$$f_k(x,t;\vec{c}) = A_k \exp(-\beta_k((c_x - w_k)^2 + c_y^2 + c_z^2)), \quad \forall\ c_y, c_z, c_{x,k} \leq c_x \leq c_{x,k+1} \tag{3.12}$$

The macroscopic governing equations are obtained by taking velocity moments:

$$\int_{c_x=c_{x,k}}^{c_{x,k+1}} \int_{c_y=-\infty}^{\infty} \int_{c_z=-\infty}^{\infty} m \left(\frac{\partial f_k}{\partial t} + c_x \frac{\partial f_k}{\partial x} = \nu(F_m - f_k) \right) dc_x dc_y dc_z$$

$$\int_{c_x=c_{x,k}}^{c_{x,k+1}} \int_{c_y=-\infty}^{\infty} \int_{c_z=-\infty}^{\infty} mc_x \left(\frac{\partial f_k}{\partial t} + c_x \frac{\partial f_k}{\partial x} = \nu(F_m - f_k) \right) dc_x dc_y dc_z$$

$$\int_{c_x=c_{x,k}}^{c_{x,k+1}} \int_{c_y=-\infty}^{\infty} \int_{c_z=-\infty}^{\infty} m(c_x^2 + c_y^2 + c_z^2) \left(\frac{\partial f_k}{\partial t} + c_x \frac{\partial f_k}{\partial x} = \nu(F_m - f_k) \right) dc_x dc_y dc_z$$

These can then be written as:

$$\frac{\partial \vec{U}_k}{\partial t} + \frac{\partial \vec{F}_k}{\partial x} = \nu(\vec{U}_k^M - \vec{U}_k) \tag{3.13}$$

where $\vec{U}_k$ is expressed as :

$$\vec{U}_k = \begin{bmatrix} \rho_k \\ \rho_k u_k \\ \rho_k e_k \end{bmatrix} = \int_{c_x=c_{x,k}}^{c_{x,k}} \int_{c_y=-\infty}^{\infty} \int_{c_z=-\infty}^{\infty} \begin{pmatrix} m \\ mc_x \\ m(c_x^2 + c_y^2 + c_z^2) \end{pmatrix} f_k dc_x dc_y dc_z$$

and $\vec{F}_k$ can be obtained by:

$$\vec{F}_k = \int_{c_x=c_{k,x}}^{c_{k+1,x}} \int_{c_y=-\infty}^{\infty} \int_{c_z=-\infty}^{\infty} \begin{pmatrix} mc_x \\ mc_x^2 \\ m(c_x^2 + c_y^2 + c_z^2)c_x \end{pmatrix} f_k dc_x dc_y dc_z$$

$\rho_k, \rho_k u_{k,x}$ and $\rho_k e_k$ are the density, momentum and energy contribution from group k respectively. $\vec{F}_k$ is the flux vector. $\vec{U}_k^M$ corresponds to the the value of $\vec{U}_k$ if β_k, w_k and A_k are replaced by the corresponding local Maxwellian distribution's values. $\vec{U}_k^M$ is the fraction of the equilibrium density, momentum, and energy that is present is the k^{th} velocity group. The factor m - mass of molecule, is present when taking moments to ensure the macroscopic

moments obtained is equivalent to density, momentum and energy equations of the Euler equations.

3.3 Macroscopic Quantities

The mathematical expressions for the group density, velocity, energy, and their corresponding fluxes in terms of the group distribution function parameters are derived in this section.

3.3.1 Function Form

A generic functional form of any group distribution function for the 1Dx-3Dv case (one dimension in physical space and three dimensions in velocity space) is given by :

$$f(x, \vec{c}, t) = A \exp(-\beta((c_x - w)^2 + c_y^2 + c_z^2)) \tag{3.14}$$

In the above equation, the spatial and temporal variations determined by the parameters β, w and A.

3.3.2 Function Definition - I_{nx}

The following notation will be used for expressing functions:

$$I_{nx} = \int_{c_x=c_i}^{c_x=c_f} (c_x - w)^n \exp(-\beta(c_x - w)^2) dc_x \tag{3.15}$$

The expressions that occur in the flux and conserved variables vector are expanded and written as follows:

$$I_{0x} = \sqrt{\frac{\pi}{4\beta}} \left(\text{erf}(\sqrt{\beta}(c_f - w)) - \text{erf}(\sqrt{\beta}(c_i - w)) \right)$$

$$I_{1x} = \left(\frac{\exp(-\beta(c_i - w)^2) - \exp(-\beta(c_f - w)^2)}{2\beta} \right)$$

$$I_{2x} = -\frac{\sqrt{\pi}}{2\sqrt{\beta}}\left(\frac{\exp(-\beta(c_f-w)^2)(c_f-w)}{\sqrt{\pi\beta}} - \frac{\exp(-\beta(c_i-w)^2)(c_i-w)}{\sqrt{\pi\beta}}\right) + (\frac{\sqrt{\pi}}{4\sqrt{\beta^3}})(\text{erf}[\sqrt{\beta}(c_f-w)] - \text{erf}[\sqrt{\beta_k}(c_i-w)])$$

$$I_{3x} = -\frac{\exp(-\beta(c_f-w)^2)(c_f-w)^2 - \exp(-\beta(c_i-w)^2)(c_i-w)^2}{2\beta} - \frac{\exp(-\beta(c_f-w)^2) - \exp(-\beta(c_i-w)^2)}{2\beta^2})$$

3.3.3 $\vec{U}$ and $\vec{F}$ expressions

The expression for $\vec{U}$ is given by:

$$\vec{U} = \begin{bmatrix} nA\frac{\pi}{\beta}I_{0x} \\ nA\frac{\pi}{\beta}(I_{1x} + wI_{0x}) \\ nA\frac{\pi}{\beta}\left(I_{2x} + w^2I_{0x} + 2wI_{1x} + \frac{I_{0x}}{\beta}\right) \end{bmatrix}$$

$$\vec{F} = \begin{bmatrix} nA\frac{\pi}{\beta}(I_{1x} + wI_{0x}) \\ nA\frac{\pi}{\beta}(I_{2x} + w^2I_{0x} + 2wI_{1x}) \\ nA\frac{\pi}{\beta}(I_{3x} + I_{0x}w^3 + 3I_{1x}w^2 + 3I_{2x}w) + \frac{nA\pi(I_{1x}+wI_{0x})}{\beta^2} \end{bmatrix}$$

3.4 Numerical Modeling

Given the governing equations, a set of initial conditions and boundary conditions, the sequence of steps used for numerical solution of the equations are

1. Divide velocity space into N_g groups and discretize space in N_x grid points
2. Note that $N_g << N_x$
3. Using the initial conditions, set the initial value of macroscopic quantities $(\rho_k, \rho_k u_k, \rho_k e_k)$ in each group at every location
4. Perform non-linear inversion using $\vec{U}_k$ to obtain function parameters for each group

5. Using function parameters, obtain the values of $\vec{F}$ for each group
6. Using a flux scheme, obtain the partial derivative of the flux vector
7. Sum up the corresponding group macroscopic values to obtain the density, temperature and velocity at each spatial location
8. Obtain the source term contribution at each location
9. Use a time stepping scheme of your choice to update solution
10. Repeat from 4 till desired time or convergence

3.5 Conclusions

The mathematical form and the numerical solution steps given summarize the key aspects required for model implementation. By solving for the moments of the Boltzmann equation, considerable computational time is saved. The underlying distribution function can be reasonably resolved using few groups in velocity space. This is because of the functional form chosen for representing the distributions. At a first glance, the derived equations are similar to the Euler equations. They behave in a similar way to Euler equations when the gas is in translational equilibrium. When the gas is not in equilibrium, the effect of the source term kicks in. Another key difference is that , the flux cannot be expressed as a function of the group macroscopic variables. This latter fact necessitates the use of a non-linear inversion routine to obtain function parameters from group macroscopic variables, which are then used to extract the flux values.

CHAPTER 4

RESULTS

Results are presented for three test cases: A zero dimensional relaxation, one dimensional shock tube problem and a one dimensional standing shock structure problem.

The zero dimensional case is chosen to study the effectiveness of the maximum entropy function formulation in resolving the distribution function in an accurate manner.

The one dimensional shock tube case is chosen as a first step to see if the model solution matches with the Boltzmann solution in a one dimensional setting.

The final simulation involving matching the structure of a one dimensional shock tries to merge the ideas in the previous runs. The shock structure requires at least a one dimensional setting and needs reasonable resolution of the distribution function for it to match the Boltzmann Solution

4.1 Zero Dimensional (Space) Relaxation

To test the accuracy of the grouping model and study the effectiveness of the inversion process a simple test case of a structure-less gas relaxing to an equilibrium distribution is studied. For this case of spatially homogeneous gas, the Krook equation Eq.(2.11) simplifies to :

$$\frac{\partial f}{\partial t} = \nu(F_m - f) \tag{4.1}$$

Eq.(4.1) can be solved analytically if the collision frequency (ν) is constant and no external energy is added into the system. The macroscopic governing

equations become:

$$\frac{\partial \rho_k}{\partial t} = \nu(\rho_k^M - \rho_k) \tag{4.2}$$

$$\frac{\partial \rho_k u_k}{\partial t} = \nu(\rho_k^M u_k^M - \rho_k u_k) \tag{4.3}$$

$$\frac{\partial \rho_k e_k}{\partial t} = \nu(\rho_k^M e_k^M - \rho_k e_k) \tag{4.4}$$

In addition to the primary goals, this model problem can be used to check the accuracy of the reconstruction of the velocity distribution using the macroscopic model parameters and macroscopic solution errors when compared against the analytical solution at intermediate time steps.

4.1.1 Initial Condition

The initial condition chosen for case 1 is a bimodal distribution in x-velocity space centered about $c_x = 0$. Such a bimodal distribution can be expressed as:

$$f_i(\vec{c}) = \frac{n}{2}\left(\frac{b}{\pi}\right)^{1.5} (\exp(-b(c_x - v)^2) + \exp(-b(c_x + v)^2)) \exp(-bc_y^2) \exp(-bc_z^2) \tag{4.5}$$

For a closed system, in the absence of energy addition, Eq.(4.5) relaxes to a Maxwellian distribution of the form:

$$F_m = n\left(\frac{b_m}{\pi}\right)^{1.5} \exp(-b_m(c_x^2 + c_y^2 + c_z^2)) \tag{4.6}$$

where

$$\frac{3}{2b_m} = \frac{3}{2b} + v^2 \tag{4.7}$$

For the test problem, velocity variables are non-dimensionalized by the mean speed of the Maxwellian and time is non-dimensionalized by the reciprocal of collision frequency ν.

The initial non-dimensionalized non-equilibrium distribution is chosen to

be a bi-modal distribution of the form:

$$f_i(\vec{c}) = \sqrt{\frac{3}{4\pi}} \left(\exp(-3(c_x - \frac{1}{\sqrt{3}})^2) + \exp(-3(c_x + \frac{1}{\sqrt{3}})^2) \right) \times \frac{3}{\pi} \exp(-3(c_y^2 + c_z^2)) \tag{4.8}$$

The corresponding Maxwellian distribution that the above non-equilibrium relaxes to is given by:

$$f_M(\vec{c}) = \frac{1}{\pi^{\frac{3}{2}}} \exp(-(c_x^2 + c_y^2 + c_z^2)) \tag{4.9}$$

The initial distribution along the x-direction and the final Maxwellian distribution that the initial distribution relaxes to are plotted in Figure 4.1.

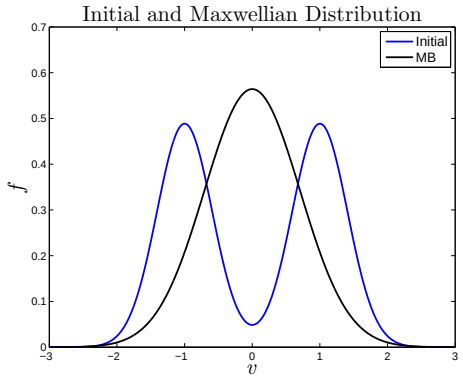

Figure 4.1: Initial distribution and corresponding Maxwell Boltzmann (MB) Distribution.

4.1.2 Results

In order to reconstruct the distribution in each group, the group density, momentum and energy equations in 4.1 are solved. The initial distribution of the gas is symmetric about the origin and continues to remain so till it reaches equilibrium. The function parameters obtained from group conserved variables are used to plot the distribution in the positive half of the velocity space.

The collision frequency ν and the number of groups N_g used in the model

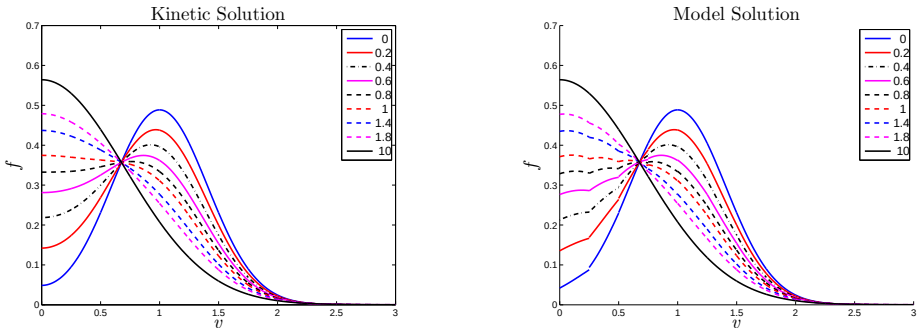

(a) Kinetic Solution (b) Model Solution

Figure 4.2: 0D Relaxation Solution at different times. Kinetic (4.2a) and Model(4.2b) solution

are:

$$N_g = 13 \tag{4.10}$$

$$\nu = 1 \tag{4.11}$$

The relaxation process is run from non-dimensional time $t = 0$ to $t = 50$. The velocity space between $0 \leq v \leq 3$ is divided into 12 equally spaced groups and the velocity space from $3 < v < \infty$ is modeled as a single group. Near the tail of the distribution, the value of the distribution function and its corresponding moments are of the order of machine precision. If more than one group is used in the tail, numerical errors occur. The macroscopic model solution in each group is independent of the solution in other groups for a BGK collision model as we assume a constant collision frequency.

The numerical solution of the multi-group maximum entropy model and the Boltzmann equation with the BGK collision operator are plotted at different times in Figs. 4.2b and 4.2a respectively. The model solution is plotted overlapping with the corresponding Boltzmann equation solution in Figure. 4.3 for 10 different times to compare the accuracy of the model solution at each intermediate time.

The model solution closely follows the exact solution. In addition, solution corresponding to a particular group is plotted over the entire velocity space. The group velocity parameter value need not lie within the group velocity bounds i.e if the group bound is $2.5 < c_{x,k} < 3$, the corresponding w_k value can be outside this bound. As time progresses, the group velocity goes from

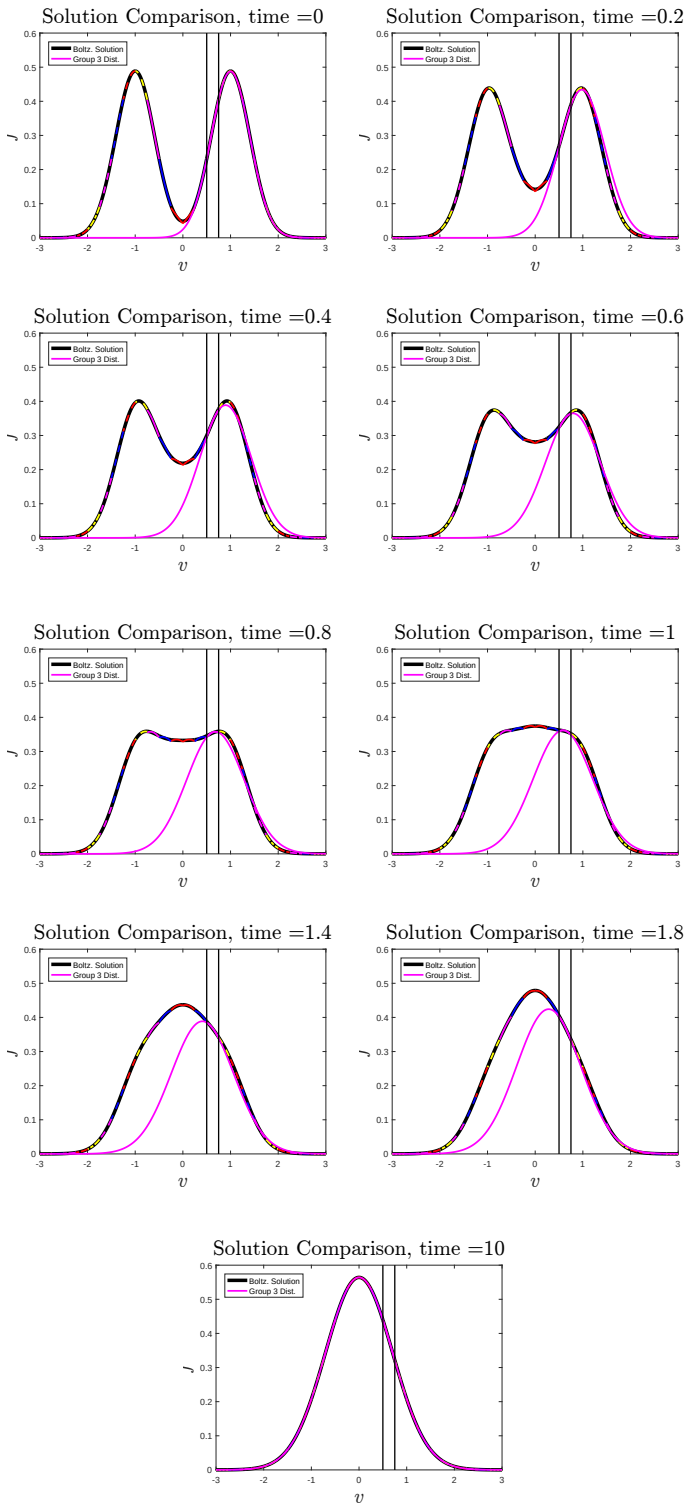

Figure 4.3: Comparison Plot - Kinetic Solution, Model Solution and Group Solution

a positive value to 0 and the group temperature increases in order to match the equilibrium solution. The final group solution and the Maxwellian at time t = 10 is identical.

One key point to note is that the model distribution function is not continuous. This does not affect the solution because the moments of the distribution are solved for instead of the distribution itself. The moments are taken only within a group and within each group the distribution is continuous. Secondly, the curvature of the group distribution function is concave. This is a consequence of the assumption that the β parameter within each group is positive. This is enforced during the non-linear solution. Since, β is equivalent to inverse temperature, its value cannot be negative and as a result, the group curvature is always concave.

Model solution obtained using 13 groups requires us to solve 39 ordinary differential equations (ODE), while the exact Krook model solution requires solving 10,000 ODE's (at each point in the discretized velocity space). This results in a reduction in the computational cost required for model solution.

Through this simple test case, it is observed that - given enough number of groups the underlying velocity distribution can be captured with reasonable accuracy. In addition, it serves as a nice test bed for the non-linear inversion routines that model algorithm uses.

4.2 One Dimensional Flow - Shock Tube

In this section, the model equations (Eq. 3.13) are used to solve the Sod Shock tube problem. The physical domain is $0 \leq x \leq 1$. The initial conditions chosen are [22]:

$$\rho_L = 1 \qquad \rho_R = 0.125 \tag{4.12}$$

$$u_L = 0 \qquad u_R = 0 \tag{4.13}$$

$$P_L = 1 \qquad P_R = 0.1 \tag{4.14}$$

$$0 \leq x \leq 0.5 \qquad 0.5 < x \leq 1 \tag{4.15}$$

where ρ is the density, P is the pressure, u is the mean flow velocity, and L, R denote the left and right half of the domain respectively. The gas parameters are non-dimensionalized by the upstream gas properties and the velocity

is non-dimensionalized by the speed of sound. Time is non- dimensionalized using characteristic time given by the fraction of the length of the domain and the speed of sound. For the initial conditions, the group function parameters are set to be equivalent to the local Maxwellian parameters The Maxwellian at each physical location can be represented by Eq. (2.6). The corresponding distribution function parameters expressed in terms of the initial conditions are:

$$n_L = \rho_L \qquad n_R = \rho_R \tag{4.16}$$

$$\beta_L = \frac{\rho_L}{2P_L} \qquad \beta_R = \frac{\rho_R}{2P_R} \tag{4.17}$$

$$u_L = 0 \qquad u_R = 0 \tag{4.18}$$

The governing equations are integrated in time using Runge Kutta fourth order time stepping method. The spatial derivatives are obtained using a 2nd order central difference scheme or characteristics based upwinding scheme. The latter scheme exploits the hyperbolic nature of the system of equations but is computationally more expensive than the central difference implementation. At the left and right boundaries, one sided stencils are used for obtaining derivatives. The test gas is assumed to have $\gamma = \frac{5}{3}$.

The model solution is compared with the corresponding kinetic solution. The kinetic solution is obtained by solving the Boltzmann equation. The specific solver used for the kinetic solution uses discontinuous Galerkin based discretizations in physical and velocity space [23, 24].

4.2.1 High Collision Frequency - Euler - Results

The velocity space is divided into three groups ($[\infty, -1], [-1, 1]$ and $[1, \infty]$). The velocity bounds shown here are the non-dimensionalized values. The x direction is discretized into 400 grid points. The time step for RK4 is taken to be 10^{-5}. The model simulation is run up-to a non dimensional time of $t = 0.2$. Within this duration, all the flow feature lie within the domain and are not affected by the boundary conditions.

The model solution was compared with the kinetic solution for two different tests - a high collision frequency ($\nu = 10000$)/low Knudsen number ($\nu \propto 1/Kn$) test case (Euler) , a low collision frequency ($\nu = 100$) case (near

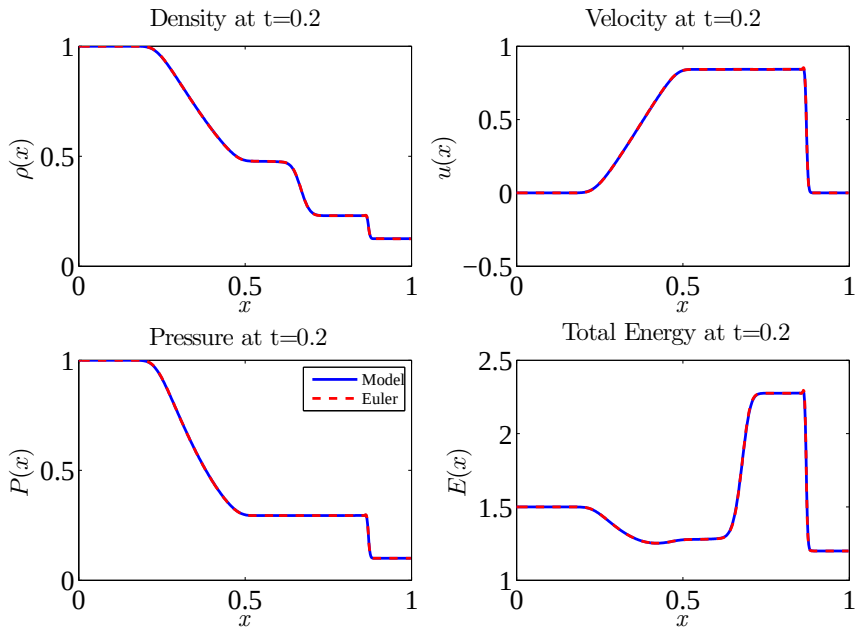

Figure 4.4: **Sod shock tube problem solution**, t = 0.2 sec, Collision Frequency $\nu = 10000$

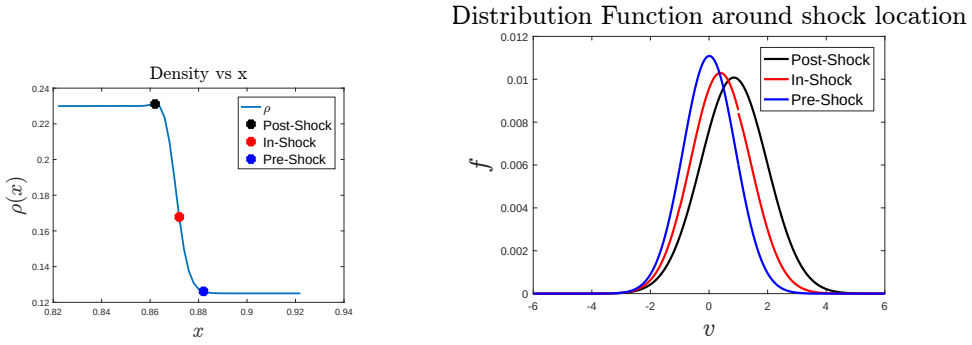

(a) Shock Schematic

(b) Distribution Function

Figure 4.5: **Distribution Function in the Shock Region,** $\nu = 10000$

end of continuum / or beginning of transition regime). Figure 4.4 shows the model results for the high collision frequency ($\nu = 10000$) case. A high collision frequency case is equivalent to the case of Euler equations. Due the high frequency of collisions occurring the molecules can quickly relax to the equilibrium distribution. The model solution is plotted alongside

the numerical solution to the Euler equations for the same set of initial conditions in Figure 4.4. The model results overlap the Euler solutions to graphic accuracy.

The distribution function within the shock is plotted for $\nu = 10000$ (Figure 4.5b). As predicted earlier, in the high collision frequency case, the distribution within the shock is Maxwellian. For this case, across the shock, the distribution smoothly goes from one Maxwellian to another.

4.2.2 Low Collision Frequency Results

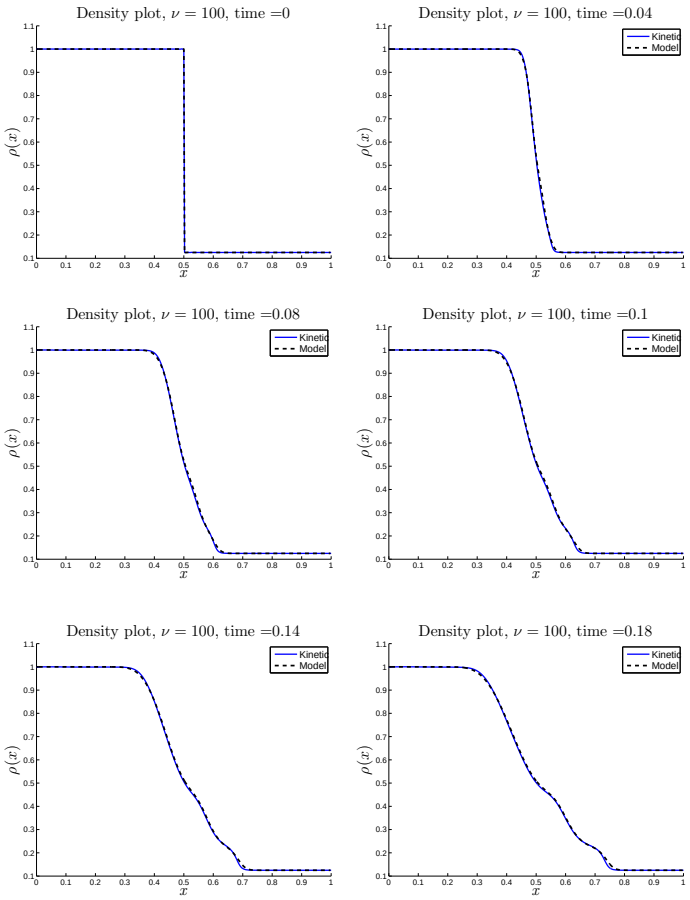

Figure 4.6: **Sod Shock Tube Problem Solution**, Collision Frequency $\upsilon = 100$, 3 groups (4.7a) - Density vs X - Time Snapshots

Next, the model solution for the case of $\nu = 100$ is compared with the corresponding Krook model simulation solution in Figure 4.7a. A low collision frequency value or a high Knudsen number corresponds to a transition

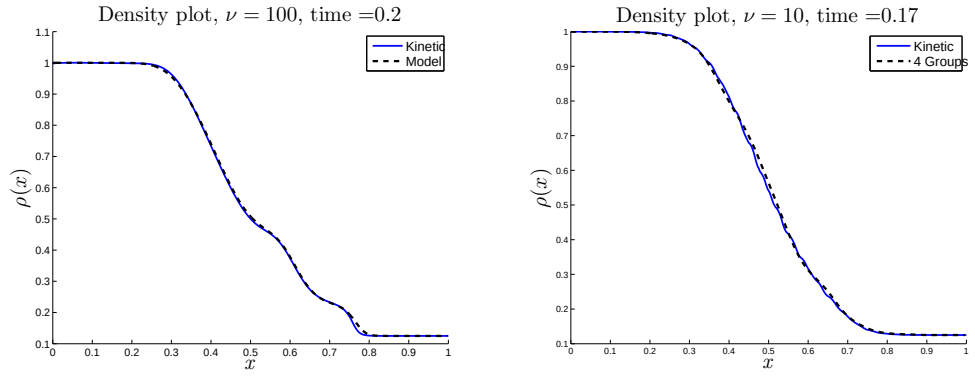

(a) Shock Tube , $\nu = 100$ case (b) Shock Tube , $\nu = 10$ case

Figure 4.7: **Sod Shock Tube Problem Solution**, Collision Frequency $\upsilon = 100$, 3 groups (4.7a), $\upsilon = 10$, 4 groups (4.7b)

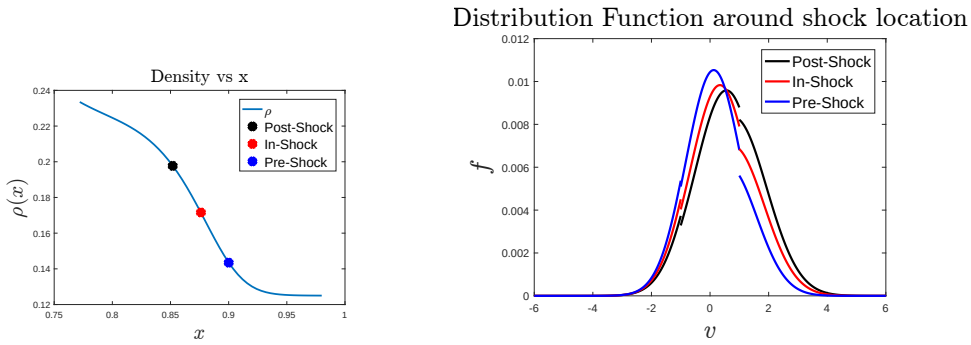

(a) Shock Schematic (b) Distribution Function

Figure 4.8: **Distribution Function in the Shock Region,** $\nu = 100$

regime. As a result, the shock and the expansion fan appear to be spread out over multiple spatial grid points in comparison to the Euler case. On further reducing the collision frequency to $\nu = 10$, we enter the rarefied gas regime. It is observed that the structures observed for the shock and expansion fan observed previously completely vanish. This is shown in (Figure. 4.7b). For collision frequency of $\nu = 10$ and lower, the velocity space needs to be divided into a larger number of groups to accurately capture the macroscopic moments. Here, we use 4 groups for $\nu = 10$.

The distribution function within the shock is plotted $\nu = 100$. (Figure

4.8b). In order non-equilibrium is captured by the model, the distribution function within the shock must be non-Maxwellian. This can be seen in (Figure 4.8b). The model does not enforce continuity of the distribution function at the group boundaries and hence jumps in the distribution function are observed. The macroscopic moments of the non-equilibrium are captured with very good accuracy using just 3 or 4 groups in velocity space. The microscopic distribution can be captured accurately if a large number of groups are used for the model. In terms of computational time, the Krook model solution takes a day to return solution while the maximum-entropy based model returns a solution in a couple of hours.

4.3 1D Standing Shock Structure

The simulation setup for this problem is similar to the shock tube case. The goal for this problem is to accurately predict the shock thickness. For this study, the thickness of a normal shock in Argon gas is studied. In order to perform comparison with corresponding shock thickness, the collision frequency is modelled using a viscosity model. Due to many issues (elaborated in the next chapter), the 1D shock structure is not exactly captured by the model. However, there a good estimate of the shock structure is obtained just using 2 groups which are presented here.

Gas	=	Argon
γ	=	$\frac{5}{3}$
$Mach_u$	=	4.0
T_u	=	300K
ρ_u	=	6.6e-6 kg/m^3
N_g	=	2
μ	=	$\mu_0 \left(\frac{T}{T_0}\right)^{0.81}$
ν	=	$\frac{P}{\mu}$
N_x	=	161

The results corresponding to the best performing case is shown in figures 4.9, 4.10, 4.11. In the results, on the right, the standing shock structure obtained from the model is compared against the Krook model solution (BGK).

At the x-location marked by the blue point on the right, the distribution function using the model function parameters and the Krook solution along the X velocity direction is plotted on the left.

The thickness of the shock is expected to increase due to the presence of non-equilibrium effects. From the plots, it is graphically observed that the shock thickness predicted by the model is lesser than the shock thickness predicted by the KrooK BGK solution. One of the reasons for this behaviour is that the underlying variation in distribution within the shock is not captured accurately. This is clearly seen through the plots on the left. The shock thickness can be captured more accurately by using greater number of groups. However, this comes at a greater computational cost and raises problems with the inversion routine used for obtaining the function parameters.

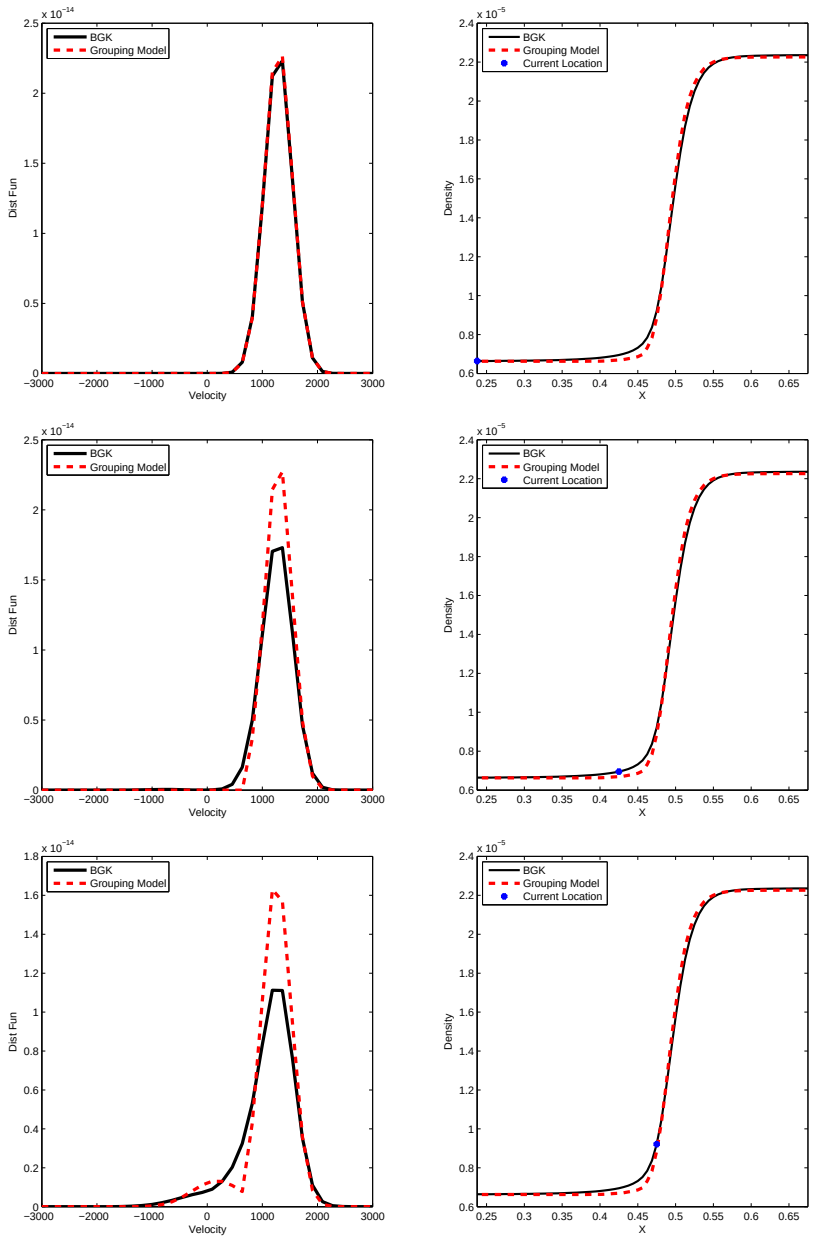

Figure 4.9: **Standing Shock** , 2 groups, Mach 4, Distribution Function as different shock location - I

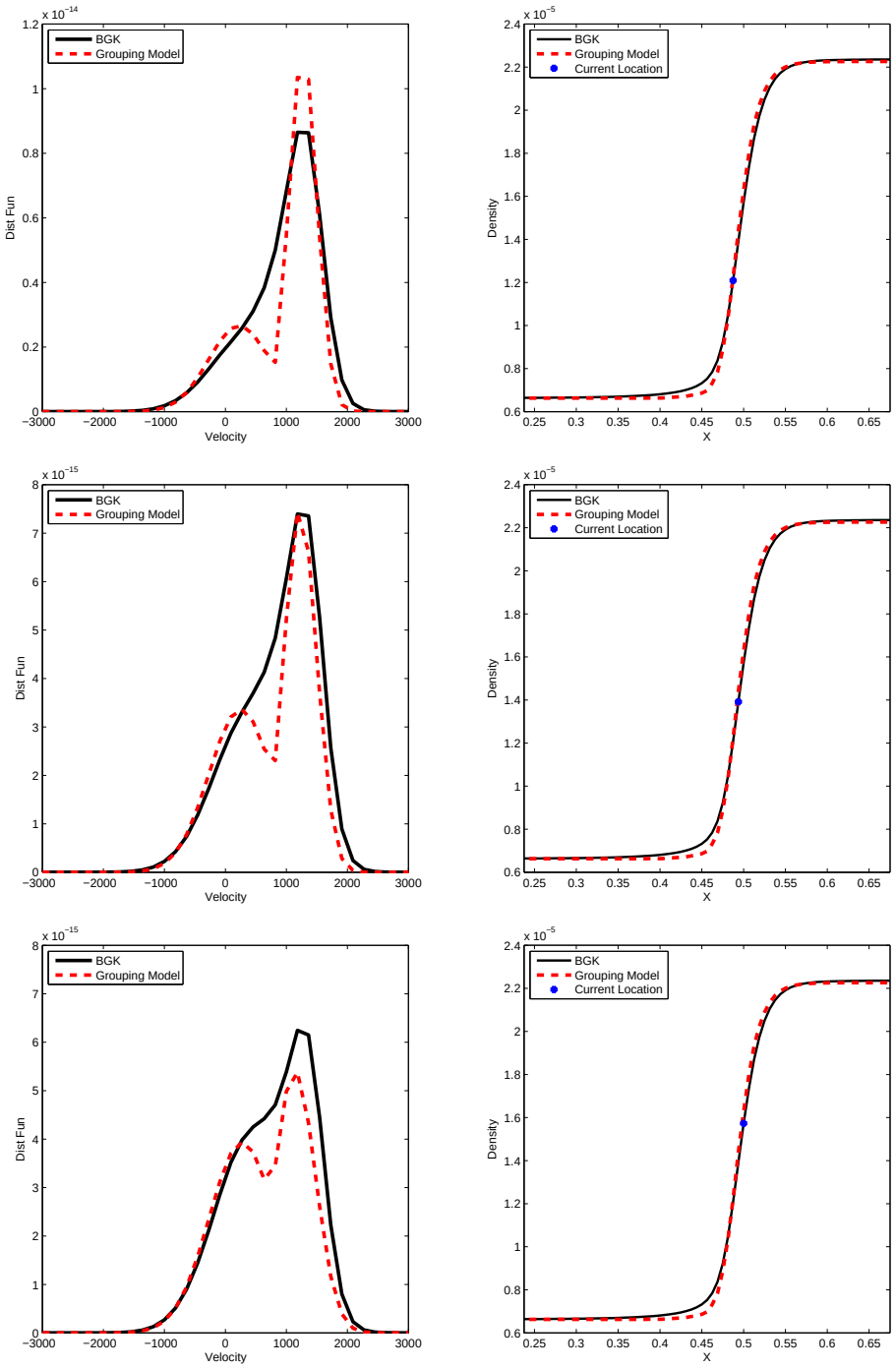

Figure 4.10: **Standing Shock** , 2 groups, Mach 4, Distribution Function as different shock location - II

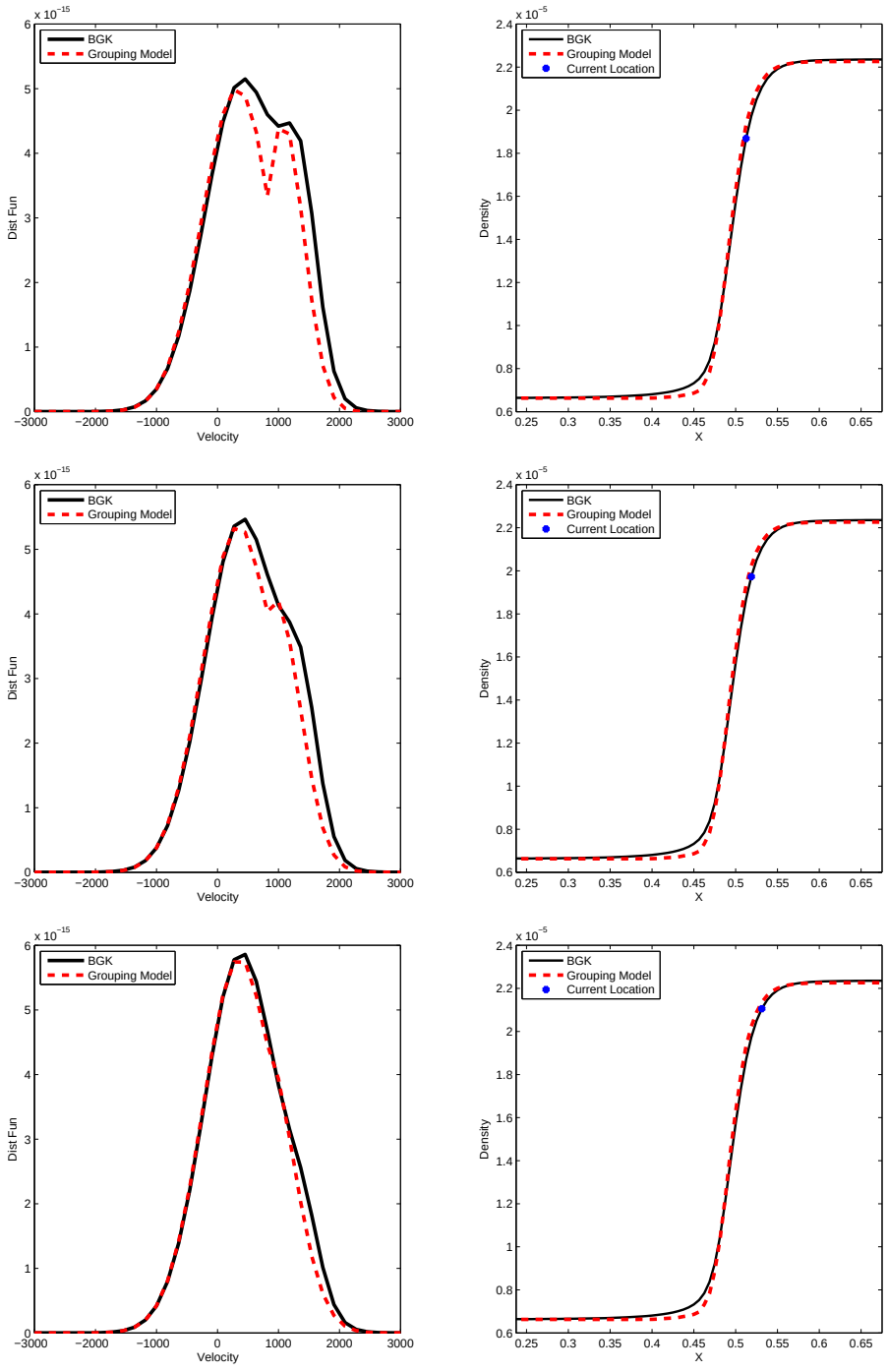

Figure 4.11: **Standing Shock** , 2 groups, Mach 4, Distribution Function as different shock location - III

CHAPTER 5

PROBLEMS AND INSIGHTS

The objective of the current work was to develop a translational non-equilibrium model that is more accurate than Navier stokes equations and not as computationally expensive as numerical models for solving the Boltzmann equations. While the model developed here satisfies the objective in principle, there are various shortcomings over the model that exist, which make it impossible to directly use the model for performing 3D spatial hypersonic flow simulations right away. In addition, over the course of working on the model, various ideas were pursued to better understand the model and capture its shortcomings. In the following sections, some problems with the current model and some open questions are elaborated. This section provides list of ideas that were attempted or considered and provide a baseline for further research in model development.

5.1 Challenges

In this section, some of the open problems that need to be addressed in order to improve the model are listed

5.1.1 Collision Integral

The general collision integral can be expressed as :

$$\left[\frac{\partial}{\partial t}(f)\right]_{coll} = \int_{-\infty}^{\infty} \int_{dP_c} [f(\vec{c}', \vec{x}, t) f(\vec{v}', \vec{x}, t) - f(\vec{c}, \vec{x}, t) f(\vec{v}, \vec{x}, t)] g dP_c dV_v \quad (5.1)$$

For the current model, moments of the collision integral is required within each group. While moments corresponding to the depleting collisions can be

handled easily, the replenishing collisions are difficult. The difficulty arises because there is no apparent relation between the groups of the colliding partners($\vec{c}$ and $\vec{v}$) and the inverse collision partners ($\vec{c}'$ and $\vec{v}'$). In the absence of such a relation, it would be difficult to get the correct contribution of the moments of the replenishing collisions within each group. This constraint, unless solved, limits the generalizabililty of the model.

In this regard, one of the first validation cases considered was replicating the results in paper by Krook and Wu [25]. However, the inability to obtain moments of the replenishing collision integral used in that paper stalled these efforts.

5.1.2 Discontinuous distributions

Existing methods for solving the Boltzmann equation numerically provide continuous distributions. While the current model, focuses on the moments and the macroscopic quantities, improvements in accuracy can be obtained by enforcing continuity. This can be done by adding additional constraints in equation 3.5

5.2 Roadblocks

In this section, a set of roadblocks that were faced during model development are elaborated. These roadblocks were not overcome during the course of work through the model development.

5.2.1 Couette Flow Problem

Couette flow problem is an alternative one-dimensional problem choice for studying translation non-equilibrium. The key aspect of Couette problem involves obtaining the variation of shear stress in a gas in a flow normal direction. There is a gradient along the y direction of $\bar{c}_x$ - the macroscopic velocity of the gas along the x direction.

However, looking at the model formulation in 3.13, there are gradients only along the x direction accounted for. If moment equations are generated along the y direction, then it would not be easy to resolve the velocity along x

direction. One possible way to circumvent the problem, would be to generate the 3Dx-3Dv equations and apply simplifications to arrive at the 1Dx-3Dv governing equations. There are some problems with this approach which are elaborated next

5.2.2 Extensions to 3D spatial equations

The expression for the group distribution function for the 1Dx-3Dv case is given by:

$$f(x, \vec{c}, t) = A \exp(-\beta((c_x - w)^2 + c_y^2 + c_z^2)) \tag{5.2}$$

A simple way to extend the function formulation for 3Dx-3Dv case would be :

$$f(x, \vec{c}, t) = A \exp(-\beta((c_x - w_x)^2 + (c_y - w_y)^2 + (c_z - w_z)^2)) \tag{5.3}$$

There are five unknown function parameters A, β, w_x, w_y, w_z. The five group macroscopic variables corresponding to density, momentum along 3 directions and energy can be used as physical constraints for extracting group function parameters.

At a first glance, above formulation works well. However, there is an inherent assumption in the above formulation which may lead to poor modeling of non-equilibrium effects. The β parameter is equivalent to inverse temperature. By constraining the group distribution function to have a single β, we are enforcing the "temperature" within a group to be equal along the three directions. This need not be true in non-equilibrium cases and can result in model performing poorly.

Alternatively, a modified function formulation is considered:

$$f(x, \vec{c}, t) = A \exp(-\beta_x(c_x - w_x)^2 - beta_y(c_y - w_y)^2 - \beta_z(c_z - w_z)^2) \tag{5.4}$$

While the above formulation solves the single temperature assumption, it is an open questions with regards to the macroscopic quantities and corresponding governing equations to be used for obtaining the parameters. There are 7 function parameters and conservation equations only provide 3 constraints. Non-physical governing equations involving cross terms can be used. However, boundary conditions cannot be specified easily for such equations and the resulting results may be non physical. In addition, the computational

cost for inverting 7 non-linear equations at every grid point is also extremely high

5.3 Standing Shock Structure - Problems

Based on the observations in the previous section, the standing shock problem still seems to be amenable to the way the model is currently constructed. The goal of the shock structure problem can be elaborated by 5.1. The pink

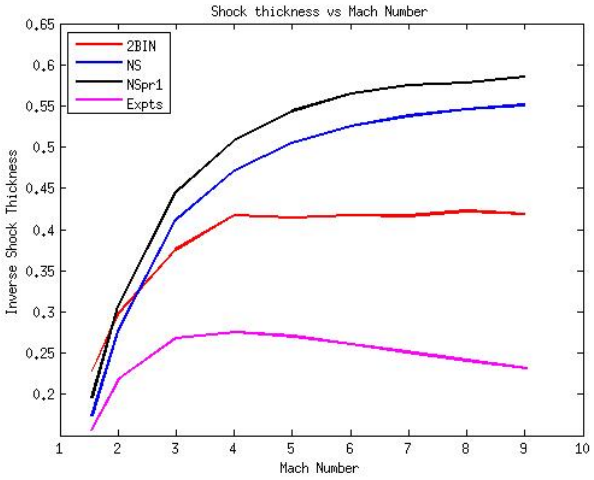

Figure 5.1: Inverse shock thickness vs Mach Number

curve represents the experimentally measured shock thickness. The model (red curve) must ideally be as close as possible to the pink curve.

The model used for generating results in Figure. 5.1 used two groups. The structure within the shock as seen in Figure 5.2 is qualitatively matching with the Krook solution. Despite this, the shock thickness is not accurately captured. In order to eliminate resolution as the reason for error in shock thickness, three groups in velocity space was used. The result for 3 group case for two different Mach numbers are shown in Figure 5.3

In Figure 5.3, there are non physical wiggles in the shock structure. It is clearly evident at higher Mach numbers, but wiggles are present in low Mach numbers as well.

While attempting to fix the wiggles and obtain better shock thickness prediction, a series of problems are identified which are listed below.

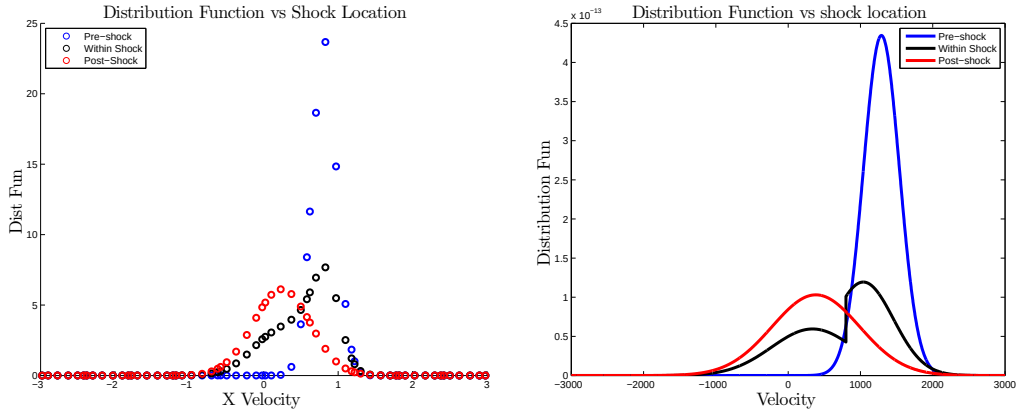

(a) Distribution function from Krook model solution

(b) Distribution function from model parameters

Figure 5.2: Distribution within shock - BGK (left) and Model (right)

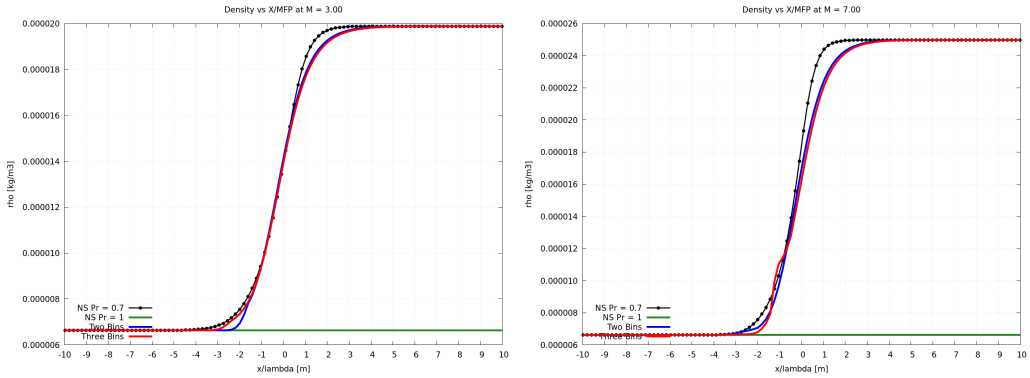

(a) Mach 3 - Density Profile

(b) Mach 7 - Density Profile

Figure 5.3: Model solution for standing shock - Problems in shock structure

5.3.1 Model inadequacy

The 1Dx-3Dv formulation, similar to the 3Dx-3Dv formulation in 5.2.2, assumes the a single "temperature" in the three velocity directions within each group. However, as clearly shown in Bird's work [26],the variation on longitudinal temperature(along x) is different from that of the variation in the lateral direction (along y and z). This could be a major contributing factor behind the shock thickness prediction errors.

5.3.2 Model Variants

Three alternatives were tried to test model efficiency

- Create a 1Dx-3Dv model with two β parameters, one along longitudinal direction and one along lateral direction similar to equation 5.4
- Try to see if model work for a simple (unrealistic) case of 1Dx-1Dv model
- Trying to test different group velocity bounds to check if it has an impact in the solution.

If a 1Dx-1Dv assumption is used, the group distribution function becomes ,

$$f(x, \vec{c}, t) = A \exp(-\beta((c_x - w)^2)) \tag{5.5}$$

While the structure of the governing equations remain the same as 3.13, the underlying expressions for $\vec{U}_k$ and $\vec{F}_k$ are no longer the same as 3.3.3 and 3.3.3. Firstly, addition β_k parameters that occur in $\vec{U}_k$ and $\vec{F}_k$ due to integration along c_y, c_z directions will vanish. In addition, the energy equation will no longer have terms that appear due to taking the $c_y^2 + c_z^2$ moments. If such an assumption is used to model a monoatomic gas like argon, the effective ratio of specific heats goes from $\gamma = 5/3$ to $\gamma = 3$

If a 1Dx-3Dv model with two β parameters is used, an additional moment equation is required for determining the additional β parameter.

All the variants tried failed to improve the solution. The shock thickness was not being accurately captured and the wiggles continued to persist in each variant. Furthermore, the solution was very sensitive to the group velocity bounds chosen when modeled using each variant. For most group velocity bounds chosen, the model did not converge. The model returned a solution (with wiggles) only when both the post and pre-shock velocity distributions had non-zero density contributions in each group. This way of group distributions is feasible for small Mach numbers. However, at higher Mach numbers there is minimal overlap of the post and pre-shock velocity distribution.

On further investigation, the reason for the all the variants of the model solutions having wiggles, sensitivity to velocity groups and inability to con-

verge for some choice of groups is - the inability of the non-linear inversion to obtain accurate function parameters from the macroscopic group moments.

5.4 Note on Inversion

One of the key steps in the numerical implementation of the model involves getting the group function parameters (A, β, w) from the group macroscopic quantities. These parameters can then be used for reconstructing the distribution in one-dimensional case and obtaining the value of the flux variables in the one-dimensional case. The expressions of group macroscopic variables $(\rho_k, \rho_k u_k, \rho_k e_k)$ in terms of the function parameters β, w are non-linear. One of the strategies considered is to normalize the group momentum and energy by the group density to eliminate A parameter and use a non-linear solver only for the other two parameters.

The Newton-Raphson algorithm or the Levenberg-Marquardt algorithm was used for finding the roots of the nonlinear equations. The former solves for the roots of the non-linear equations while the latter casts the root finding as a minimization problem.

The primary culprit for most of the model failures during simulation are the error functions present the group density expressions. Error function reach their asymptotic value of ± 1. This phenomena explains the high sensitivity of model solution to group velocity bounds. If the group velocity bounds are such that one of the post/pre shock distributions have low density components in the group, the error functions representing the group density variable quickly saturates, causing problems with inversion. This is because low density values result in round-off errors that corrupt the normalization Another technique attempted involved generating a lookup table to obtain β and w given the normalized group energy and group velocity. The surface plot showing β and w_k is shown in Figure 5.4. From the plots,we see that points cluster at specific edges of the surface (shown by the closely spaced lines at the left and right edges of Figure 5.4a and the left edge of Figure 5.4b). At these edge locations, the group density is extremely low. the surfaces in Figure 5.4 are interpolated and the interpolated values are used for distribution function reconstruction or flux evaluation.

A summary of some of the techniques are attempted for improving the

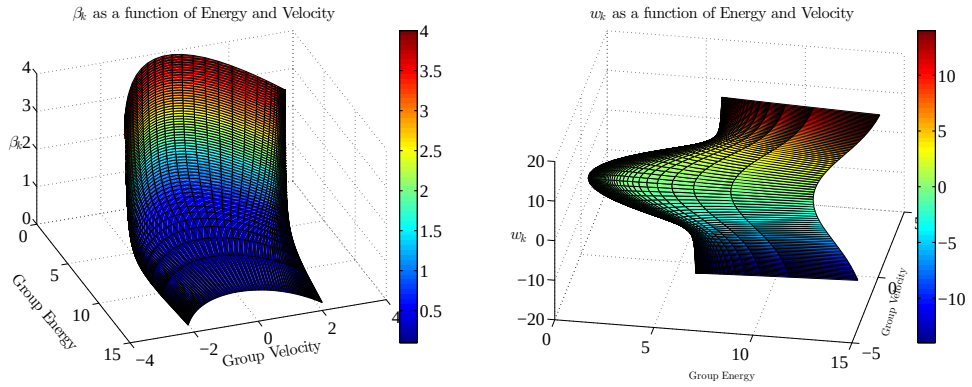

(a) β_k surface plot

(b) w_k surface plot

Figure 5.4: Inversion Surface Plots , β_k or w_k as function of normalized group energy and velocity

reliability of inversion are:

- Storing a history of parameter values to serve as good initial guess for non-linear solver
- Non-dimensionalizing the macroscopic variables and function parameters to
- Supplying the Navier Stokes solution as an initial condition for group macroscopic parameters
- Attempted 3 parameter inversion (A, β, w) and two parameter inversion (β, w) to see if any improvements can be obtained
- Fixing the solution of erroneous parameters with last known correct parameter value
- Using minimization routines like trust-region-dogleg or Levenberg-Marquardt algorithm to see if they can perform the non-linear inversion better

Among these methods, the best performing case was using a Levenberg-Marquardt method with two parameter inversion was the only method that did not cause the solution to diverge. Even this method, resulted in wiggles being observed in the shock structure. On further investigation, the wiggles

are present because of the inability of the non-linear inversion to improve the solution beyond a certain point. Over the course of the simulation (before the shock structure reaches a steady state), if the intermediate value of the macroscopic moments are such that the group density is very low or if an intermediate step in the non-linear inversion iterations, the error function inputs become large enough to saturate the output, the non-linear inversion fails.

5.5 Conclusion

A multi-group maximum entropy model for modeling flows with translational non-equilibrium is developed. The performance of the model on a zero-dimensional relaxation, one dimensional moving shock and one-dimensional standing shock is observed. Some of the key advantages of the model are its ability to capture non-equilibrium effects at significantly lower computational cost and the physical motivation underlying the model development. Key disadvantages of the model pertain constraints that need to be overcome to generalize the model to three dimensional settings and crippling dependence of the model to non linear inversion. A wide variety of open questions, problems faced during the model development and persisting errors are elaborated. All of the points mentioned can serve as fertile ground for future research.

REFERENCES

[1] P. A. Gnoffo, "Planetary-entry gas dynamics 1," *Annual Review of Fluid Mechanics*, vol. 31, no. 1, pp. 459–494, 1999.

[2] W. G. Vincenti and C. H. Kruger, "Introduction to physical gas dynamics," *Introduction to physical gas dynamics, by Vincenti, Walter Guido; Kruger, Charles H. New York, Wiley [1965]*, vol. 1, 1965.

[3] S. Chapman and T. G. Cowling, *The mathematical theory of non-uniform gases: an account of the kinetic theory of viscosity, thermal conduction and diffusion in gases*. Cambridge university press, 1970.

[4] E. Fatemi and F. Odeh, "Upwind finite difference solution of boltzmann equation applied to electron transport in semiconductor devices," *Journal of Computational Physics*, vol. 108, no. 2, pp. 209–217, 1993.

[5] F. Filbet and G. Russo, "High order numerical methods for the space non-homogeneous boltzmann equation," *Journal of Computational Physics*, vol. 186, no. 2, pp. 457–480, 2003.

[6] A. Alekseenko and E. Josyula, "Deterministic solution of the spatially homogeneous boltzmann equation using discontinuous galerkin discretizations in the velocity space," *Journal of Computational Physics*, vol. 272, pp. 170–188, 2014.

[7] G. A. Bird and J. Brady, *Molecular gas dynamics and the direct simulation of gas flows*. Clarendon press Oxford, 1994, vol. 5.

[8] H. Grad, "On the kinetic theory of rarefied gases," *Communications on pure and applied mathematics*, vol. 2, no. 4, pp. 331–407, 1949.

[9] C. D. Levermore, "Moment closure hierarchies for kinetic theories," *Journal of statistical Physics*, vol. 83, no. 5-6, pp. 1021–1065, 1996.

[10] Y. Liu, M. Panesi, A. Sahai, and M. Vinokur, "General multi-group macroscopic modeling for thermo-chemical non-equilibrium gas mixtures," *The Journal of chemical physics*, vol. 142, no. 13, p. 134109, 2015.

[11] M. Torrilhon, "Modeling nonequilibrium gas flow based on moment equations," *Annual Review of Fluid Mechanics*, vol. 48, pp. 429–458, 2016.

[12] Y. Liu, M. Vinokur, M. Panesi, and T. Magin, "A multi-group maximum entropy model for thermo-chemical nonequilibrium," *AIAA paper*, vol. 4332, p. 2010, 2010.

[13] N. Crouseilles, P. Degond, and M. Lemou, "A hybrid kinetic/fluid model for solving the gas dynamics boltzmann–bgk equation," *Journal of Computational Physics*, vol. 199, no. 2, pp. 776–808, 2004.

[14] B. Dubroca and A. Klar, "Prise en compte d'un fort déséquilibre cinétique par un modèle aux demi-moments," *Comptes Rendus Mathematique*, vol. 335, no. 8, pp. 699–704, 2002.

[15] V. Jayaraman, Y. Liu, and M. Panesi, "Multi-group maximum entropy model for translational non-equilibrium," in *47th AIAA Thermophysics Conference*, 2017, p. 4024.

[16] P. L. Bhatnagar, E. P. Gross, and M. Krook, "A model for collision processes in gases. i. small amplitude processes in charged and neutral one-component systems," *Physical review*, vol. 94, no. 3, p. 511, 1954.

[17] H. W. Liepmann, R. Narasimha, and M. T. Chahine, "Structure of a plane shock layer," *The Physics of Fluids*, vol. 5, no. 11, pp. 1313–1324, 1962.

[18] C. E. Shannon, "A mathematical theory of communication," *ACM SIGMOBILE Mobile Computing and Communications Review*, vol. 5, no. 1, pp. 3–55, 2001.

[19] E. T. Jaynes, "Information theory and statistical mechanics," *Physical review*, vol. 106, no. 4, p. 620, 1957.

[20] M. Arroyo and M. Ortiz, "Local maximum-entropy approximation schemes: a seamless bridge between finite elements and meshfree methods," *International journal for numerical methods in engineering*, vol. 65, no. 13, pp. 2167–2202, 2006.

[21] L. R. Mead and N. Papanicolaou, "Maximum entropy in the problem of moments," *Journal of Mathematical Physics*, vol. 25, no. 8, pp. 2404–2417, 1984.

[22] G. A. Sod, "A survey of several finite difference methods for systems of nonlinear hyperbolic conservation laws," *Journal of computational physics*, vol. 27, no. 1, pp. 1–31, 1978.

[23] A. Alekseenko and E. Josyula, "Deterministic solution of the spatially homogeneous boltzmann equation using discontinuous galerkin discretizations in the velocity space," *Journal of Computational Physics*, vol. 272, pp. 170–188, 2014.

[24] A. Alekseenko, "Numerical properties of high order discrete velocity solutions to the bgk kinetic equation," *Applied Numerical Mathematics*, vol. 61, no. 4, pp. 410–427, 2011.

[25] M. Krook and T. T. Wu, "Exact solutions of the boltzmann equation," *Physics of Fluids (1958-1988)*, vol. 20, no. 10, pp. 1589–1595, 1977.

[26] G. Bird, "The velocity distribution function within a shock wave," *Journal of Fluid Mechanics*, vol. 30, no. 3, pp. 479–487, 1967.